RSC Advances

PAPER

View Article Online
View Journal | View Issue

Cite this: *RSC Adv.*, 2022, **12**, 36012

Colorimetric/photothermal dual-mode sensing detection of ascorbic acid based on a Ag[I] ion/3,3′,5,5′-tetramethylbenzidine (TMB) system

Ya Di, † Jiyao Zheng,† Yunwang Zhao, Zikai Yang, Changshun Xie, Jiahan Yu, Yue Zheng * and Liming Gao*

In this work, a novel strategy of colorimetric and photothermal dual-mode sensing determination of ascorbic acid (AA) based on a Ag^+/3,3′,5,5′-tetramethylbenzidine (TMB) system was developed. In this sensing system, Ag^+ could oxidize TMB with a distinct color change from colorless to blue color, strong absorbance at 652 nm and a photothermal effect under 808 nm laser irradiation due to the formation of oxidized TMB (oxTMB). When AA was present, oxTMB was reduced accompanied by a change from blue to colorless, and a decrease in absorption peak intensity and the photothermal effect. AA concentration showed a negative linear correlation with the value of both the absorbance intensity at 652 nm and temperature in the range of 0.2–10 μM ($A = -0.03C + 0.343$ (R^2, 0.9887; LOD, 50 nM); $\Delta T = -0.57C + 8.453$ (R^2, 0.997; LOD, 7.8 nM)). Based on this, a sensing approach for detection of AA was proposed with dual-mode and without the complicated synthesis of nanomaterials. The photothermal effect and colorimetric signal provided a dual-mode detection strategy for AA, overcoming the limitations of any single mode. This colorimetric and photothermal dual-mode detection has great potential in the detection of AA in clinical pharmaceuticals and the construction of portable and highly sensitive sensors.

Received 26th October 2022
Accepted 3rd December 2022

DOI: 10.1039/d2ra06770f

rsc.li/rsc-advances

1 Introduction

Ascorbic acid (AA) is known as vitamin C, and is an effective antioxidant against numerous oxidative diseases including cardiovascular disease, various sorts of cancers, AIDS, mental illness and so on.[1] AA can remove free radicals of oxygen, nitrogen and sulphur to prevent DNA, amino acid residues and lipids from being oxidized which would induce cancers and various disorders.[2] Furthermore, AA levels are related to many diseases. For example, higher levels of AA can lead to undesired kidney stones,[3] diarrhea and stomach cramps.[4] On the other hand, inadequate intake of AA causes scurvy and anemia,[5] and affects the immune system and protein metabolism.[6] Therefore, it is of great significance to develop appropriate and operative methods to detect AA in medicines, food, and blood serum.

To date, various methods have been employed to measure AA including electrochemistry,[7] chromatography,[8] colorimetry[9] and fluorescence.[10] Colorimetry is currently the focus due to its simplicity and low cost based on facile determination by monitoring the color with the naked eye and/or measuring the optical intensity by UV-vis spectroscopy. 3,3′,5,5′-tetramethylbenzidine (TMB), due to its different color in the reduced (colorless) and oxidized (blue) forms, is usually used in colorimetric assays. Specifically, the oxidized form of TMB, oxTMB, exhibits a distinctive absorption peak at 652 nm.[11] Li *et al.*[12] prepared cobalt-doped carbon quantum dots (Co-CQDs) with peroxidase-mimetic activity, which could convert colorless and transparent TMB into blue oxTMB with dissolved oxygen, to detect AA (10–400 μM) with a LOD of 0.27 μM. Zheng *et al.*[13] synthesized a metal–organic framework, MOF-808, which could effectively catalyze the oxidation of TMB when H_2O_2 served as an oxidant. When AA was present, due to its significant inhibition effect, a significant color variation happened in the solution and facile colorimetric sensing of AA was successfully established. The AA detection limit was 15 μM, and the linear range was 30–1030 μM. Although great progress in nanomaterial/TMB systems for detection of AA has been made, they still suffer from some drawbacks such as tedious preparation, and poor stability and biocompatibility of the nanomaterials. Fortunately, some groups have reported that Fe^{3+}, Ag^+, ClO^-, and so on, could also oxidize TMB to form oxTMB with variation of color and typical absorption peak intensity at 652 nm.[14–16] Therefore, it can be predicted that based on these, a simple colorimetric method for the determination of AA would be obtained. On the other hand, colorimetric sensing has only been used for qualitative and semi-quantitative analysis because of the low resolution and different color perceptions of individuals. Recently, photothermal sensors have been extensively explored based on different photothermal responsive materials which could resolve the limitation of conventional

The First Hospital in Qinhuangdao Affiliated to Hebei Medical University, Qinhuangdao 066004, China. E-mail: yuezheng1965@sina.com

† These authors contributed equally.

colorimetric sensors. Interestingly, oxTMB also exhibits strong near-infrared (NIR) laser-driven photothermal efficiency and could be used as a highly sensitive photothermal reagent to translate the detection signal into a heat signal to obtain quantitative photothermal detection. Fu *et al.*[17] proposed an iron oxide-induced TMB–H_2O_2 colorimetric system to achieve photothermal and visual quantitative detection of prostate-specific antigen (PSA) with a low concentration (1.0 ng mL^{-1}) in normal human serum.

Herein, we reported a colorimetric and photothermal dual-mode sensor for detection of AA based on a Ag^+/TMB system. The Ag^+/TMB reaction system exhibited a distinct blue color, strong absorbance at 652 nm and a photothermal effect under 808 nm laser irradiation due to the formation of oxTMB. When AA was present, oxTMB was reduced with a change from blue to colorless, and a decrease in both absorption peak intensity and the photothermal effect. The visual colorimetric and quantitative photothermal strategy overcame the limitations of any single mode and exhibited great potential in clinical detection of AA.

2 Materials and methods

2.1 Materials and regents

Ascorbic acid (AA) was obtained from Shanghai Zhongqin Chemical Reagent Co. Ltd (Shanghai, China). 3,3,5,5-Tetramethylbenzidine (TMB), and $AgNO_3$, were purchased from Aladdin Chemistry Co. Ltd (Shanghai, China). All other chemicals were of analytical grade and all aqueous solutions were prepared by using deionized water (>18.25 MΩ cm). A pen-style digital thermometer (detection range of −50 °C to +300 °C) was purchased from a local supermarket.

2.2 Colorimetric and quantitative photothermal assay for AA

In the typical colorimetric and quantitative photothermal detection of AA, 100 μL of TMB (0.4 mM) and 100 μL Ag^+ (0.4 mM) were added into 100 μL NaAc–HAc buffer solution (0.2 M, pH 4.0), and incubated at room temperature for 20 min. Then, 100 μL AA with different concentrations was added to the Ag^+/TMB system and left for 15 min. To investigate the colorimetric sensing and quantitative photothermal performance, a UV-vis spectrometer and a thermometer were used under 808 nm laser irradiation at 2.0 W.

3 Results and discussion

3.1 The mechanism and feasibility of the sensing system

The mechanism of sensing detection of AA based on Ag^+/TMB as the colorimetric probe and photothermal reagent is shown in Scheme 1. A previous paper has reported that Ag^+ could oxidize colorless TMB to form blue oxTMB, which exhibited strong absorption at 652 nm.[18] Introduction of AA into the Ag^+/TMB system resulted in fading of the blue color and a decrease in the absorbance. This could be attributed to oxTMB being reduced to TMB as in the following equations:

$$Ag^+ + TMB \rightarrow Ag + oxTMB \quad (1)$$

$$oxTMB + AA \rightarrow TMB + DHAA + H^+ \quad (2)$$

A controlled experiment was carried out to prove this mechanism. 0.4 mM Ag^+ was added into 0.4 mM TMB and 0.2 M HAc–NaAc buffer (pH 4.0) at room temperature. Then, 0.1 mM AA was added to the above mixture and the absorption is shown in Fig. 1(A). The pure TMB solution (black line) exhibited no obvious absorption peak, however, a strong and obvious absorption peak at 652 nm was observed for the Ag^+/TMB mixture solution (red line) due to the formation of oxTMB, accompanied by a color change of the solution from colorless to blue. When AA was added, a sharp decrease in absorbance (blue line) and obvious color fading occurred, which demonstrated that oxTMB could be reduced by AA. Moreover, oxTMB showed strong light absorption at 652 nm (NIR region) which suggested that our colorimetric reaction system, Ag^+/TMB, might convert the color signal to a thermal one. Different component systems

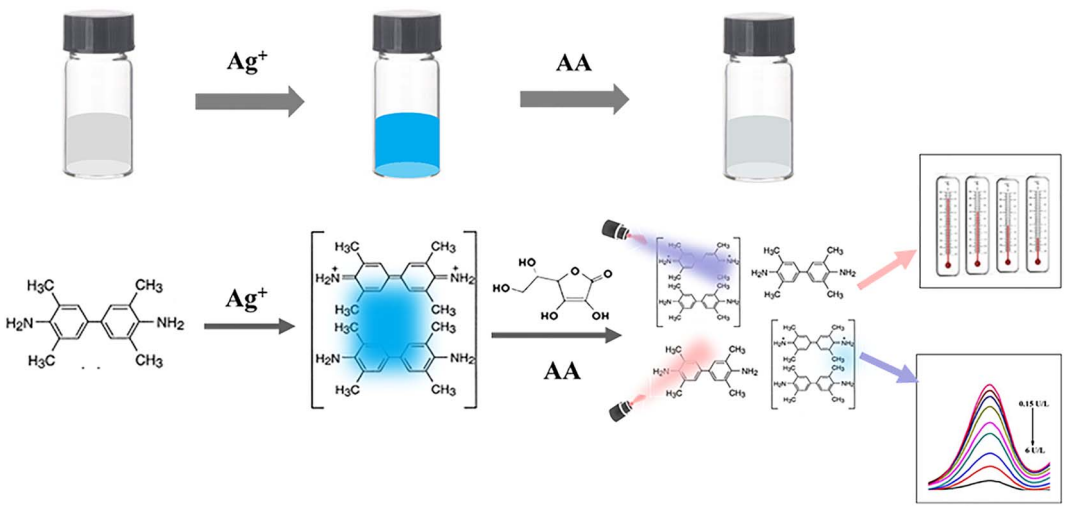

Scheme 1 Schematic illustration of the principle of colorimetric and photothermal detection of AA using the Ag^+/TMB system.

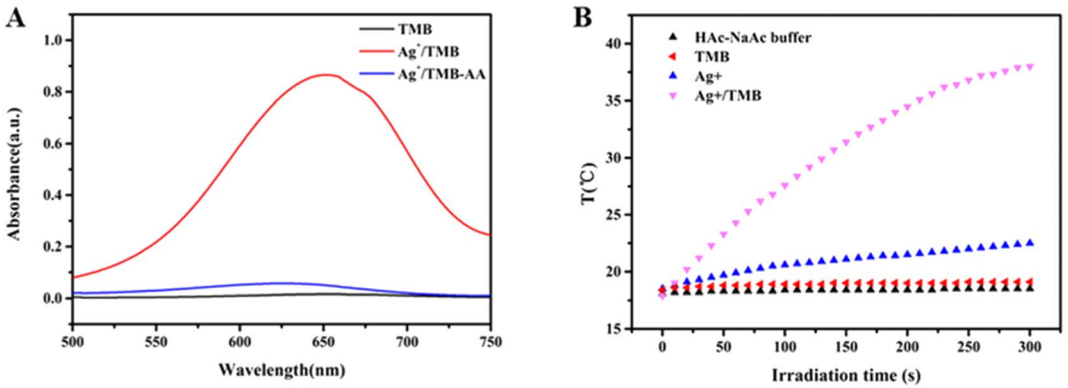

Fig. 1 (A) UV-vis absorption spectra of TMB, Ag^+/TMB, and Ag^+/TMB-AA; (B) temperature increase of HAc–NaAc buffer, TMB, Ag^+ and Ag^+/TMB.

including HAc–NaAc buffer, TMB, Ag^+ and Ag^+/TMB were exposed under an 808 nm laser at a power of 2.0 W for 60 s to investigate the photothermal effect using a digital thermometer as shown in Fig. 1(B). The Ag^+/TMB colorimetric system exhibited a dramatic temperature increase of about 20.0 °C, however, HAc–NaAc buffer, TMB, and Ag^+ showed no significant temperature increments.

These investigations proved that Ag^+/TMB could be an excellent photothermal reagent due to its photothermal conversion ability in the NIR region. Therefore, the detection of AA using Ag^+/TMB as the colorimetric probe was feasible.

3.2 Optimization of detection conditions

To obtain an excellent detection performance, some experimental conditions including pH, reaction temperature, incubation time and Ag^+ concentration were investigated. The effect of reaction temperature on the absorbance intensity of oxTMB at 652 nm was tested between 25 and 50 °C, as shown in Fig. 2(A). At the beginning, with the temperature increasing, the intensity of absorbance peaks increased. When the temperature reached 40 °C, the maximal absorbance intensity was achieved. As the temperature increased further, there was almost no change in absorbance intensity. Therefore, 40 °C was chosen as the reaction temperature. Meanwhile, as we know, pH influences the oxidase activity of Ag^+, that is, too high or too low pH is not beneficial for the oxidase reaction of Ag^+/TMB. As Fig. 2(B) shows, the absorbance intensity increased when the pH increased between 3.2 and 4.6, however, the absorbance intensity decreased when the pH was higher than 4.6. Therefore, pH 4.6 was used in the next experiments. The effect of incubation time was investigated as

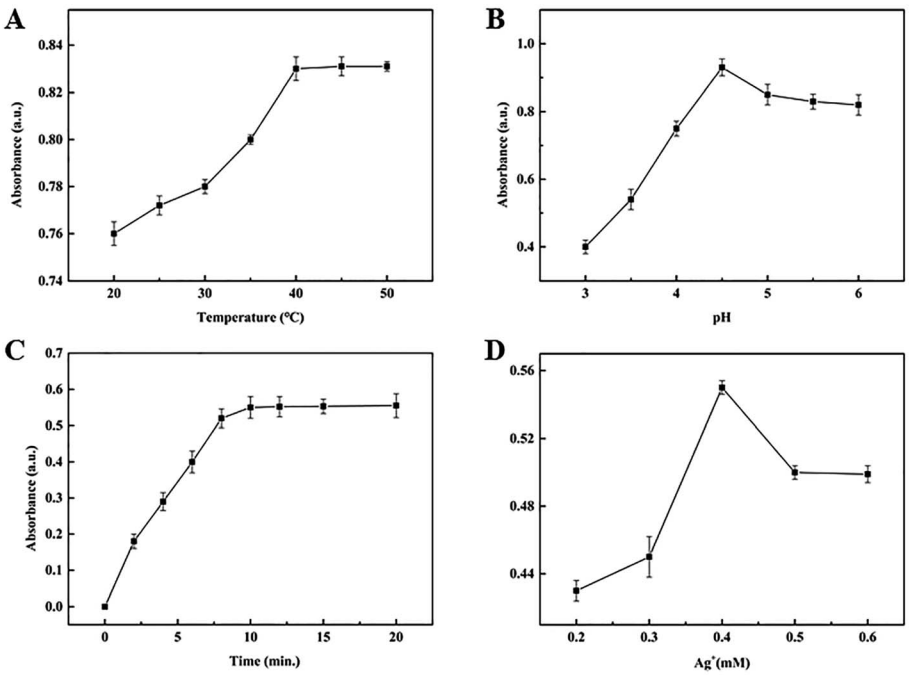

Fig. 2 The effects of (A) reaction temperature; (B) pH; (C) incubation time; (D) Ag^+ concentration.

shown in Fig. 2(C) in the range from 0–20 min. The absorbance intensity of oxTMB increased rapidly between 0 and 10 min. But for more than 10 min, the absorbance intensity of oxTMB increased slightly as the incubation time was extended. 10 min was chosen as the optimum incubation time. Another important parameter was Ag^+ concentration which is shown in Fig. 2(D). The results indicated that when the concentration of Ag^+ was higher than 0.4 mM, the absorbance intensity of oxTMB at 652 nm decreased. We predicted that the product of single-electron oxidation was further oxidized to form the double-electron oxidation product and excessive or low concentration of Ag^+ was not suitable for AA determination. Consequently, 0.4 mM Ag^+ concentration was adopted as the optimum concentration in the following detection experiments.

3.3 AA detection performance

A sensitive visual and quantitative approach for detecting AA was constructed based on the relationship between the absorbance intensity of oxTMB and AA concentration as shown in Fig. 3(A). When AA was present, the absorbance of oxTMB at 652 nm gradually decreased with increasing AA concentration. Furthermore, a negative linear correlation was present between the AA concentration and absorbance at 652 nm in the range of 0.2–10 μM, and the linear equation was $A = -0.03C + 0.343$ (C, AA concentration) with a coefficient of determination (R^2) of 0.9887 and a LOD of 50 nM (S/N = 3) (Fig. 3(B)). This linear relationship provided a basis to link the detection information from the colorimetric readout to the photothermal effect of oxTMB for AA detection. The photothermal effect of this colorimetric system was also investigated using a thermometer (Fig. 3(C)). As the concentration of AA increased, the temperature of the oxTMB solutions decreased for irradiation times from 10 to 180 s, which may result from the decreasing concentration of oxTMB as the photothermal reagent. Moreover, the temperature decrease was proportional to the concentration of AA in the range from 0.2 to 10 μM from 10 s to 60 s, however, the linear relationship changed beyond 60 s, which might be due to the photobleaching of oxTMB under longer-term irradiation.[17] Thus, 60 s was chosen as the optimal irradiation time which would avoid the photobleaching of oxTMB. The linear correlation was $\Delta T = -0.57C + 8.453$ with an R^2 of 0.997 and a LOD of 7.8 nM (S/N = 3), which indicated a high sensitivity compared with previous reports as shown in Table 1.

The influences of potential interferents, including Ca^{2+}, Cd^{2+}, Co^{2+}, Fe^{2+}, Hg^{2+}, Mg^{2+}, Mn^{2+}, Pb^{2+}, glutathione (GSH), L-cysteine and dopamine (DA) were also investigated for both colorimetric and photothermal detection as shown in Fig. 4(A) and (B). No obvious changes were found in both absorbance and in temperature when AA coexisted with interferents, which demonstrated that the as-proposed sensing system possessed excellent selectivity toward AA.

3.4 Application in real samples

To validate the reliability of this developed method, it was employed to detect pharmaceutical products containing AA from different pharmaceutical companies (Vitamin C tablets:

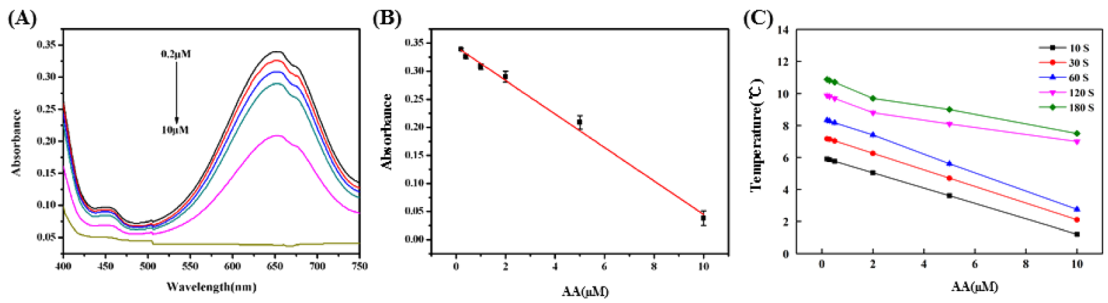

Fig. 3 (A) UV-vis spectra of different amounts of AA for this sensor. (B) Relationship between the absorbance and the AA concentration. (C) Temperature decrease for different irradiation times *versus* the concentration of AA.

Table 1 Previous reports of various analytical assays for AA sensing detection

Methods	Sensing system	Linear range (μM)	LOD (μM)	Ref.
Colorimetry	CQDs/TMB/H_2O_2	10–70	3.26	19
Fluorimetry	NaYF,Yb,Tm@$NaYF_4$/CoOOH	0–60	0.2	20
Colorimetry	MoS_2/NC/TMB/H_2O_2	0.2–80	0.12	21
Electrochemistry	Bi_2S_3/rGO	5.0–1200	2.9	22
Colorimetry	ClO/TMB	1–70	0.58	23
Colorimetry	MIL-68	3–40	0.256	24
Colorimetry	Co-POP/TMB	20–400	1.6	25
Colorimetry	Ag^+/TMB	0.2–10	0.05	This work
Photothermal	Ag^+/TMB	0.2–10	0.0078	

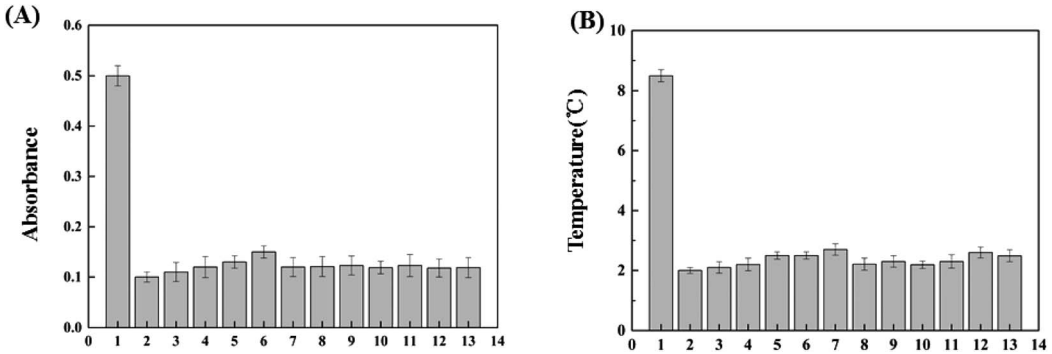

Fig. 4 The absorbance (A) and temperature changes (B) of this Ag^+/TMB system with various ions. The concentration of AA and other interferents is 4 μM. Error bars show the standard deviations of three independent experiments. 1, Blank (Ag^+/TMB); 2, AA; 3 to 13 denote AA with other interferents, namely Ca^{2+}, Cd^{2+}, Co^{2+}, Fe^{2+}, Hg^{2+}, Mg^{2+}, Mn^{2+}, Pb^{2+}, glutathione (GSH), L-cysteine and dopamine (DA), respectively.

Table 2 Detection of AA in clinical medicines

		Colorimetric assay			Photothermal assay		
	Spiked (μM)	Found (μM)	Recovery (%)	RSD (%)	Found (μM)	Recovery (%)	RSD (%)
1	2.0	2.040	102.0	2.15	2.038	101.9	2.21
2	5.0	4.990	99.8	1.06	5.020	100.4	3.20
3	10.0	10.220	102.2	3.58	9.990	99.9	3.30

Sample 1 purchased from Kunming Zhenhua Medical Co., Ltd, Kunming, China; Sample 2 purchased from Anhui City Co., Ltd, Hefei, China; Sample 3 purchased from Northeast Pharmaceutical Group Shenyang First Pharmaceutical Co. Ltd, Shenyang, China). The medicines were diluted with 20 mM PBS (pH 5.6) and the standard addition method was carried out as shown in Table 2. The recoveries were between 99.8% and 102.2% with relative standard deviation (RSD) less than 5%. The results indicated that the visual and quantitative method based on the Ag^+/TMB system was high precision and reliable for pharmaceutical sample detection.

4 Conclusions

In conclusion, we proposed a colorimetric and photothermal dual-mode sensor for detection of AA using a Ag^+/TMB system. This sensor depended on Ag^+ oxidizing colourless TMB to form a blue reaction product (oxTMB), which could act as a colorimetric probe and photothermal reagent. When oxTMB was reduced by AA, both the absorbance and temperature of the sensing system showed a negative linear correlation with AA concentration in the range of 0.2–10 μM ($A = -0.03C + 0.343$ (R^2, 0.9887; LOD, 50 nM); $\Delta T = -0.57C + 8.453$ (R^2, 0.997; LOD, 7.8 nM)). Based on these, a colorimetric and photothermal evaluation system for AA was obtained. The photothermal effect and colorimetric signal provided a dual-mode detection strategy for AA, overcoming the limitations of any single mode. Moreover, detection of AA in pharmaceuticals showed the great potential of this sensing approach in clinical detection.

Author contributions

Conception and design: J. Zheng; funding support: Y. Zheng, L. Gao; methodology: Ya Di; data analysis: Y. Zhao, Z. Yang; writing: C. Xie, J. Yu; administrative, technical, or material support: Liming Gao; final approval of manuscript: Y. Zheng and L. Gao. All authors read and approved the final manuscript.

Conflicts of interest

There are no conflicts to declare.

Acknowledgements

This work was financially supported by the Key Research and Development Plan of Hebei Province [No.203777114D] and the Medical Science Research Project of Hebei Province [No. 20221611].

Notes and references

1 Z. Chen, Y. Huang, D. Cao, S. Qiu, B. Chen, J. Li, Y. Bao, Q. Wei, P. Han and L. Liu, *Front. Nutr.*, 2022, **8**, 812394.
2 M. J. González, J. R. Miranda-Massari, E. M. Mora, A. Guzmán, N. H. Riordan, H. D. Riordan, J. J. Casciari, J. A. Jackson and A. Román-Franco, *Integr. Cancer Ther.*, 2005, **4**, 32–44.
3 W. Xu, J. Chen, S. Sun, Z. Tang, K. Jiang, L. Song, Y. Wang, C. Liu and H. Lin, *Nanoscale*, 2018, **10**, 17834–17841.

4 X. Zhu, T. Zhao, Z. Nie, Y. Liu and S. Yao, *Anal. Chem.*, 2015, **87**, 8524–8530.
5 L. K. Massey, M. Liebman and S. A. Kynast-Gales, *J. Nutr.*, 2005, **135**, 1673–1677.
6 M. Sabatier, A. Rytz, J. Husny, S. Dubascoux, M. Nicolas, A. Dave, H. Singh, M. Bodis and R. P. Glahn, *Nutrients*, 2020, **12**, 2776.
7 K. Liu, P. Yu, Y. Lin, Y. Wang, T. Ohsaka and L. Mao, *Anal. Chem.*, 2013, **85**, 9947–9954.
8 I. Klimczak and A. Gliszczyńska-Świgło, *Food Chem.*, 2015, **175**, 100–105.
9 J. Chen, J. Ge, L. Zhang, Z. Li, J. Li, Y. Sun and L. Qu, *Microchim. Acta*, 2016, **183**, 1847–1853.
10 J. Wang, X. Peng, D. Li, X. Jiang, Z. Pan, A. Chen, L. Huang and J. Hu, *Microchim. Acta*, 2018, **185**, 1–8.
11 S. Kim, J. Lee, S. Jang, H. Lee, D. Sung and J. Chang, *Biochem. Eng. J.*, 2016, **105**, 406–411.
12 C. Li, J. Zeng, D. Guo, L. Liu, L. Xiong, X. Luo, Z. Hu and F. Wu, *ACS Appl. Mater. Interfaces*, 2021, **13**, 49453–49461.
13 H.-Q. Zheng, C.-Y. Liu, X.-Y. Zeng, J. Chen, J. Lü, R.-G. Lin, R. Cao, Z.-J. Lin and J.-W. Su, *Inorg. Chem.*, 2018, **57**, 9096–9104.
14 Y. Guo, Q. Ma, F. Cao, Q. Zhao and X. Ji, *Anal. Methods*, 2015, **7**, 4055–4058.
15 S. Liu, J. Tian, L. Wang and X. Sun, *Sens. Actuators, B*, 2012, **165**, 44–47.
16 L. Zhang and J. Du, *Spectrochim. Acta, Part A*, 2016, **158**, 24–28.
17 G. Fu, S. T. Sanjay, W. Zhou, R. A. Brekken, R. A. Kirken and X. Li, *Anal. Chem.*, 2018, **90**, 5930–5937.
18 M. Luo, X. Xue, H. Rao, H. Wang, X. Liu, X. Zhou, Z. Xue and X. Lu, *Sens. Actuators, B*, 2020, **309**, 127707.
19 S. Chandra, V. K. Singh, P. K. Yadav, D. Bano, V. Kumar, V. K. Pandey, M. Talat and S. H. Hasan, *Anal. Chim. Acta*, 2019, **1054**, 145–156.
20 Y. Cen, J. Tang, X.-J. Kong, S. Wu, J. Yuan, R.-Q. Yu and X. Chu, *Nanoscale*, 2015, **7**, 13951–13957.
21 J. Zheng, D. Song, H. Chen, J. Xu, N. S. Alharbi, T. Hayat and M. Zhang, *Chin. Chem. Lett.*, 2020, **31**, 1109–1113.
22 C. Qu, H. Li, S. Zhou, G. Li, C. Wang, R. Snyders, C. Bittencourt and W. Li, *Chemosensors*, 2021, **9**, 190.
23 C. Mu, H. Lu, J. Bao and Q. Zhang, *Spectrochim. Acta, Part A*, 2018, **201**, 61–66.
24 J.-W. Zhang, H.-T. Zhang, Z.-Y. Du, X. Wang, S.-H. Yu and H.-L. Jiang, *Chem. Commun.*, 2014, **50**, 1092–1094.
25 D. Guo, C. Li, G. Liu, X. Luo and F. Wu, *ACS Sustainable Chem. Eng.*, 2021, **9**, 5412–5421.